Spatial quantification of vegetation density from terrestrial laser scanner data for characterization of 3D forest structure at plot level

Durrieu[1] S., Allouis[1] T., Fournier[2] R., Véga[1] C., Albrech[1] L.

[1]UMR TETIS Cemagref/Cirad/ENGREF-AgroParisTech, Maison de la Télédétection, 34093 Montpellier Cedex 5, France,
sylvie.durrieu@teledetection.fr, tristan.allouis@teledetection.fr,
cedric.vega@teledetection.fr, laurent.albrech@teledetection.fr
[2]Centre d'Applications et de Recherche en Télédétection, Université de Sherbrooke, Sherbrooke (Québec) Canada, Richard.Fournier@USherbrooke.ca

Abstract

Precise description of forest 3D structure at plot level is required for sustainable ecosystem management. However, a detailed structure description from traditional field measurements is tedious. We propose an innovative method to quantify in 3D the spatial distribution of forest structure from terrestrial lidar data. The method rests on the hypothesis that the normalized number of laser returns within a given volume element is proportional to the density of vegetation material inside this volume. The developed model is based on analysis made inside Svoxels (spherical voxels) to compute a spatialized vegetation density index. The model was tested on two different scans of the same plot. The resulting vegetation density index well represents the vegetation structure as observed within the lidar point cloud. Quantitative analyses confirmed a global consistency of the results within and between scans. However, we observed a slight bias in the computed density indexes. It might be mainly explained by occlusions, which cause 1) a slight decrease of the density index with distance and 2) local differences in density index between scans. Future work will focus on improving our algorithm and correcting biases. These results are promising for the development of quantitative measures of the 3D forest structure.

Keywords: Terrestrial lidar, forest canopy, 3D model, architecture, stand structure

1. Introduction

Precise description of 3D structure of forests is useful for timber resource monitoring, ecosystem management and preservation, or improved understanding on ecosystem functioning. However the spatial complexity of forests makes structure measurement very difficult, particularly since structure is not a satisfyingly defined feature (Fleck *et al.* 2007). A complete 3D plot description is not conceivable using traditional field inventory methods. The recent development of terrestrial lidars allows to acquire very detailed 3D data on forest structure. It opens up new opportunities to derive metrics closely linked to forest structure and to reduce time and costly field measurements (Hopkinson *et al.* 2004).

Terrestrial lidars were originally developed for civil engineering (see Lichti *et al.* (2002) for examples of systems and applications). Recent studies expanded their use on tree or stand structure measurements. Most of them focused on estimating traditional field-based forest parameters. Hopkinson *et al.* (2004) first demonstrated that it is possible to locate and identify individual trees with high precision and to measure total tree height and diameter at breath height (dbh). Tree heights were however underestimated of about 1.5 m when compared with field validation data. This was mostly due to low sampling density at the upper canopy level

caused by occlusion effects of the signal and a suboptimal survey protocol. Results for mean dbh differed by only 1 cm from tape measurements. Similar results were obtained by other authors for both height and dbh measurements using semi-automatic data extraction methods (Watt and Donoghue 2005; Fleck *et al.* 2007; Wezyk *et al.* 2007). Other forest parameters such as stem density, total basal area, gross and merchantable timber volume were also estimated from terrestrial lidar data with a good agreement when compared with traditional field measurements (*e.g.* volume estimations within 7 % of the traditional field estimations (Hopkinson *et al.* 2004)). Other efforts dealt with automatic tree location and height, dbh, stand basal area or timber volume estimations (Aschoff *et al.* 2004; Bienert *et al.* 2007; Király and Brolly 2007; Wezyk *et al.* 2007).

The very high sampling rate of terrestrial laser systems allows to generate detailed 3D canopy models therefore opening up the possibility to analyze fine scale stand structure, foliage distribution, canopy light transfer or leaf area indices that are important to understand and model forest function and dynamic. However few studies have demonstrated the interest of such systems for ascertaining parameters beyond those from the traditional inventories. As an exception, Fleck *et al.* (2007) proposed a method to quantify canopy projection far much precise than the 8-point canopy projection from a ground operator used in traditional inventories. As other non-traditional measures, Danson *et al.* (2007) proposed a method to estimate canopy directional gap fraction and Van der Zande *et al.* (2006) an approach for vegetation profile reconstruction. Studies using terrestrial lidar show much opportunity for developing new methods for forest canopy metrics that will take full advantage of terrestrial lidar datasets. One of the main issues will be to solve the problem of the distance-dependent varying point density from the lidar returns.

This paper introduces an innovative approach to analyze the vegetation structure from 3D point clouds acquired with terrestrial lidar. The method quantifies the 3D spatial distribution of forest canopy material in volume elements (~dm level). It makes available operational calculations linking the 3D point cloud recorded by a terrestrial lidar with the spatial distribution of the vegetation. This study was also performed considering the link between airborne lidar and field data with the aim of improving information extraction from airborne lidar data on forested areas. Indeed airborne lidars proved capable to estimate the spatial distribution of forest parameters such as height, crown area, timber volume or biomass at both tree or stand level (Lim *et al.* 2003). However these airborne estimates require local calibration through acquisition of field data.

2. Method

2.1 Study area and field data

The main study site is part of a National Environmental Observatory (ORE Draix) located in the southern part of the French Alps. It is part of the Haute-Bléone state forest, mainly composed of black pine (*Pinus nigra*) planted in the 1880's to protect against soil erosion. Most of the stands are even-aged and mature. Elevations range from 802 to 1263 m. Traditional field inventory was conducted during December 2007 within circular plots of 15 m and 9 m radius. Within the plot the following characteristics were measured for all the trees with dbh > 7 cm: dbh, total and timber heights, crown base height, crown diameter and tree position. For the purpose of that study, we focused on a 15 m circular plot having a tree density of 66 stems/ha and located on a flat area.

2.2 Data acquisition with the terrestrial lidar

Terrestrial lidar surveys were made on March 2008 using an ILRIS-3D system (Optech Inc,

Toronto, Canada). The system measures the laser returns within a window 40° wide in both horizontal and vertical directions. The laser emits and measures light at 1,500 nm. Point density of each scan is controlled by the operator. The system can register the intensity and distance for either the first or the last backscattered signal. In our study, we selected primarily the last returns considering that they would provide a better statistical representation of the vegetation distribution compared with first returns. However, first and last returns were recorded at some particular system base stations (*i.e*. system location) for comparison and quality assessment. The ILRIS-3D base stations were selected outside the plot at varying distance from the plot centre and separated by an angle of about 120° relating to the plot center. Artificial targets (polystyrene spheres with 8 cm diameter) were distributed within the plot and measured using differential GPS and total station to improve the alignment (co-registration) and the georegistration of the scans acquired from different base stations.

2.3. Method developed for quantifying the spatial distribution of vegetative elements

The objective of this study was to develop an algorithm to calculate vegetation density from lidar returns visible in the form of point clouds. The point density needs to be locally transformed into density of vegetation components. We used a statistical approach hypothesizing that the interception rate is related to the vegetation density. Such an approach was preferred to a formal physical-based model (e.g. Beer-Lambert law) because of the heterogeneity of distribution of canopy components and also because of the relatively small footprint of the laser beam compared to vegetation elements size. Estimation of density index throughout a scene involved first dividing the plot-space into constant volume elements (voxels). For each voxel, we calculated (1) the number of lidar points within the voxel and (2) the number of laser beams entering the voxel. The density index of each voxel is given by the ratio (1) / (2). Our method has two spatial characteristics: a regularly spaced grid of voxel centers and the use of spherical voxels.

2.3.1. Regular 3D grid and spherical voxels

Voxel centers were arranged on a 3D grid regularly distributed along x, y and z axes. The grid was georeferenced in the Lambert III conformal conic coordinate system and was used to process each scan of a same plot. Computations from all scans of the plot could therefore be compared and integrated. Before processing each scan, the Lambert III grid is changed into the Cartesian system of the scan. The transformation model is computed using (1) The Lambert III coordinates of target centers, measured on the field (total station + DGPS), and (2) the Cartesian coordinates of the targets, measured on each scan by fitting a spherical shape on its corresponding point clouds. The 3D Reshaper ® software was used for that purpose. A minimum of 4 spheres was required for computing the transformation model.

Data acquisition with the terrestrial lidar follows a spherical geometry. We therefore adopted a spherical geometry to simplify computations on the resulting point cloud from lidar measurements. Lidar position was taken as the origin of the spherical system. The space illuminated by the lidar was already divided into voxels. Therefore each voxel center was associated with a spherical coordinate (r, θ, φ) and bounded with the following conditions:

1. 4 angles: $\theta_{min} = \theta - d\theta$, $\theta_{max} = \theta + d\theta$, $\varphi_{min} = \varphi - d\varphi$ and $\varphi_{max} = \varphi + d\varphi$,
2. 2 distances: $r_{min} = r - dr$, $r_{max} = r + dr$,

with dr set to half the grid resolution. This new volume is referred to as the spherical voxel or Svoxel (Figure 1). We set $d\theta$ and $d\varphi$ to ensure a constant volume of Svoxels ($V = R^3$, with R the 3d resolution of the grid). The resulting Svoxels have the following properties:

1. Distortion of a Svoxel compared to the reference voxel is proportional to r (cf. figure 1),
2. Distortion of a Svoxel increases when angles θ and φ increase,
3. Svoxels are not strictly contiguous. Small overlaps or gaps can occur which are more

important for larger values of θ and φ,

4. For a given center point, the Svoxels generated from different base station locations will not strictly overlap due to slight changes in shape and orientation. The highest differences will occur when comparing Svoxels from scan with a 45° (modulo 90°) difference between viewing angles.

Even with these properties, differences between voxels and Svoxels remain small and it is thus assumed that they are not detrimental to precise density index computation.

Figure 1: Shape of a Svoxel at 1 m (a) and at 3 m (b) for 50 cm grid resolution.

2.3.2 Algorithm to calculate density index of the grid points

The following algorithm was implemented to calculate the density index of each Svoxel in the lidar scanning field of view:

1. Generation of a 3D regularly spaced grid in Lambert III at a resolution R,
2. Projection of the grid in the sensor Cartesian system,
3. Switch scan point cloud and grid into spherical system,
4. For each point of the grid :
    1. Computation of the theoretical number of laser beams ($N_{theorical}$) entering the Svoxel based on the point density selected for the scan. This number decreases with distance to the sensor due to the scanning geometry.
    2. Evaluation of the number of laser beams intercepted before the targeted Svoxel (N_{before}: points satisfying the 4 angles equation with a distance lower than r_{min}). The difference between $N_{theorical}$ and N_{before} represents the number of beams reaching the Svoxel.
    3. Identification of the number of returns inside the targeted Svoxel (N_{inside}: points satisfying the 4 angles and 2 distances equations).
    4. Computation of the vegetation density index D, such as:

$$D = N_{inside} / (N_{theorical} - N_{before})*100 \quad (1)$$

    If $N_{theorical} - N_{before} = 0$, a no-data value is assigned. If $N_{theorical} - N_{before}$ is lower than a given threshold Ts, results are considered as non-significant because too few beams are available to assess Svoxel density. Output of results in Lambert III.
5. Steps 2 to 5 can be reapplied to other scans of a same plot acquired from other base stations.

2.4 Data analysis and validation

For this preliminary study the algorithm was applied on 2 out of the 8 scans available for the plot. Scan density was set to 6.24 mm (resp. 7.02 mm) at 15 m for scan 1 (resp. scan 2) and the last returns were recorded. Three Svoxel resolutions were selected: 0.25, 0.5 and 1 m. Results

were first evaluated from a preliminary visual assessment where Svoxels with a positive and significant density index were visualized on the lidar 3D point clouds of selected trees. Preliminary tests allowed us to adopt a value of 50for the threshold defined for non-significant values (Ts).

Then two sets of procedures were realized:

1. In order to evaluate the result consistency inside a given scan, several stand crowns located at various distances from the base station 1 were extracted and the distribution of positive and significant density indices were analyzed. Results on four black pines and one Spanish fir (*Abies pinsapo*) were compared (cf. Fig 2).
2. Density index values obtained from two different base stations were also compared to evaluate the consistency of the results between different scans. This preliminary analysis defined if results from multiple scans can be compared and merged.

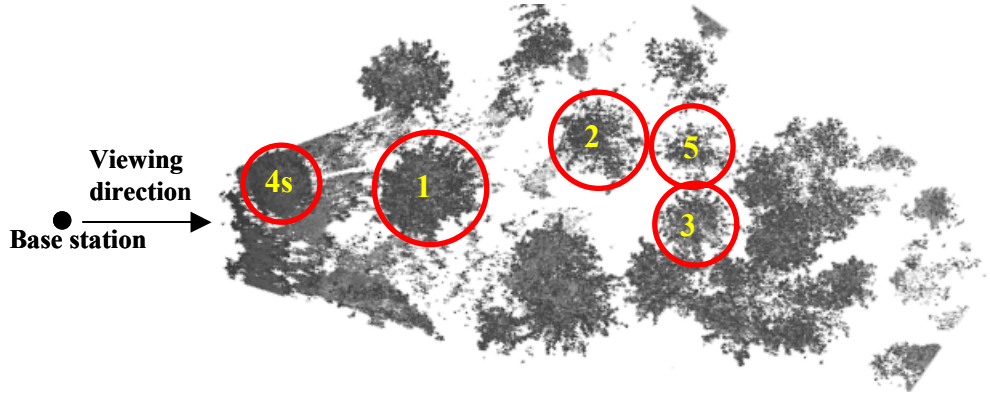

Figure 2: The tree crowns selected for analysis are shown on the 3D point cloud obtained from the system position 1 and viewed from the top. Crowns represent black pine (1, 2, 3 and 5) and Spanish fir (4).

3. Results and discussion

3.1 Visual analysis

The method gave visually consistent results. Figure 3 compares the point cloud from the original scan and the values of the density index for Svoxels on a vertical slice of a black pine crown. The tree shape is well described by Svoxels with density index values apparently reasonable: highest density values are logically located along the trunk and close to large branches regardless of the Svoxel size. Tree outline description quality is getting coarser when Svoxel size increases. However decreasing the Svoxels size increases the rate of non-described areas (no-data Svoxels) of the crown due to occlusions (i.e. mutual shading) particularly at the back part of the tree. Therefore researches have to be conducted to define the Svoxel size providing the optimal description of the vegetation structure. The optimal Svoxel size is expected to vary with the stand structure (density, tree dimensions and tree arrangement). Furthermore the number of beams generated by the lidar should be high enough to allow enough intercepted beams by the tree structures of the scene. While the point density at each Svoxel varies greatly according to the scanning parameters and the occlusion effects between canopy elements, the computed density indexes are relatively homogeneous within the crowns. The link between spatial distribution of canopy components and density index of Svoxels follows the general density patterns expected for these conifers. However, a slight dissymmetry remains between density index of Svoxels of the crown facing the scanner system and those on the back part of the tree. This may be explained by a heterogeneous spatial distribution of vegetation

elements. The occlusion of some vegetation elements may bias the density index values (Fig. 4). At tree level, underestimation and overestimation effects do not offset each other inducing a slight underestimation towards the back of the crown (Fig. 3).

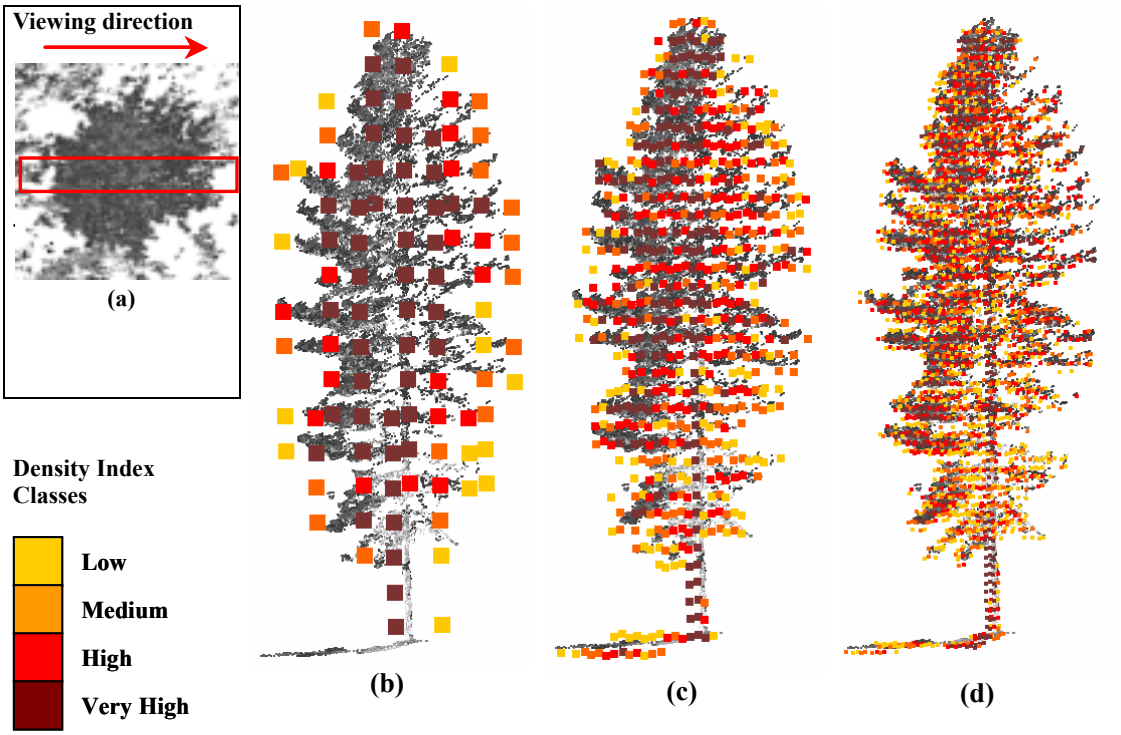

Figure 3: Density index were computed for the three grid dimension (0.25, 0.5, 1m). Density index are superimposed on their corresponding Svoxel centre on the lidar 3D point cloud. Results are given for a slice cut through a tree in the scan direction (a). Density index were separated into 4 classes using quartiles.

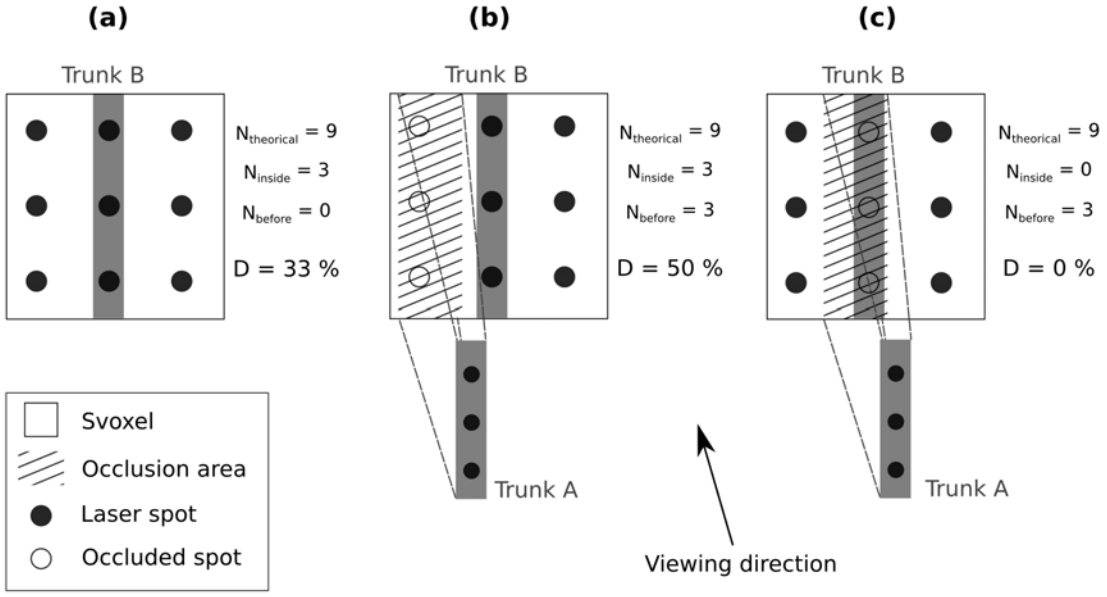

Figure 4: Effect of occlusion on the density index: (a) When Trunk B in the Svoxel is hit by 3 beams out of 9 it leads to a density index of 33 %. (b) When Trunk A external to the Svoxel is hit by 3 incoming beams but does not mask another canopy element in the Svoxel, the density index becomes 50 %. (c) When Trunk A masks trunk B and no other vegetation components is hit in the Svoxel, the density index is 0 %.

3.2 Comparative analysis of different tree crowns in a same scan

Results for the five selected trees are summarized in table 1. The number of Svoxels with a positive and significant density index gives an indication of the number of Svoxels used for computing each mean tree density index. It varies significantly from one tree to another and cannot be simply related to distance from the lidar system. This number depends on Svoxel size, tree size, distance from the sensor and occlusion patterns. As for the mean density values, we expected similar values for a same species. Although values were relatively similar for the 4 black pine trees (table 1), their mean density index varied respectively from 10 to 13.4 %, 9.8 to 12.8 % and 8.3 to 14.6 % for the 25 cm, 50 cm and 1 m Svoxel resolutions respectively. Since only few trees were analyzed this could be due to natural tree heterogeneity. However, further tests on more trees are required to validate if a bias could originate from occlusion effects, similarly as what was observed for the density index in front and towards the back of individual crowns. In such case density index would decrease with the amount of obstacles in the path of the light beams. This trend can be observed from our dataset for all Svoxel resolutions but not very clearly (table 1). For instance when comparing results for black pine 3 and 5, tree mean index is clearly affected by the vegetation present between the lidar system and the observed tree: black pine 3, is less affected by occlusions (see figure 2) than black pine 5 and has a higher density index (table 1). We hypothesize that occlusions of the incident beams might be the main contributor to this bias. The anomalies related to the distance probably result from (1) a decrease of the sampling density with distance to the lidar system and (2) a change in the spatial distribution of the laser beams entering the Svoxels. Occlusions transform the regular sampling pattern into an irregular. In heterogeneous middles, this transformation may biased the density index computation. Additional analyses are necessary to evaluate the incidence of this bias on the quality of vegetation characterization. Combining scans acquired from various base stations will allow to quantify and partly correct this bias.

Table 1: For each tree crown density index mean and standard deviation were computed for 3 grid resolutions: 25, 50 and 100 cm. The theoretical entering beam number gives an indication of the crown distance from the lidar system.

Svoxel resolution		Spanish fir 4s	Black Pine 1	Black Pine 2	Black Pine 3	Black Pine 5
Distance		15 m	21 m	33 m	39 m	39m
25 cm	Number of Svoxel with significant positive value inside the crown	3455	7328	1172	1558	457
	Mean $N_{theorical}$	1821	585	285	212	214
	Mean density index	**14.2**	**12.9**	**13.4**	**11.4**	**10.0**
	(standard deviation)	*(15.1)*	*(14.0)*	*(14.8)*	*(13.1)*	*(13.2)*
50 cm	Number of Svoxel with significant positive value inside the crown	705	1859	777	566	349
	Mean $N_{theorical}$	7199	2317	1103	840	829
	Mean density index	**15.9**	**12.8**	**11.3**	**10.5**	**9.8**
	(standard deviation)	*(15.7)*	*(12.8)*	*(12.1)*	*(11.5)*	*(12.8)*
1 m	Number of Svoxel with significant positive value inside the crown	136	396	244	136	116
	Mean $N_{theorical}$	28405	9271	4380	3354	3288
	Mean density index	**17.8**	**14.6**	**11.0**	**10.8**	**8.3**
	(standard deviation)	*(18.4)*	*(14.0)*	*(11.3)*	*(11.7)*	*(9.6)*

Histograms of the density index values allow to compare the distribution for the 5 selected crowns for the three grid resolutions. Figure 5 presents the histogram for a Svoxel grid resolution of 50 cm. The histograms are comparable for all the pines. For the Spanish fir a slight difference can be noticed on figure 5 and was observed at all the 3 resolutions: density index frequencies are higher than those from the pines for densities ranging from 20 to 50. Consequently standard deviations were similar for all the black pine crowns and were higher for the Spanish fir (table 1). A higher foliage density for this species could explain this result, even if the density index computation bias is likely to contribute to this difference. This open up the possibility to classify species using density index distribution.

3.3 Comparison of density index for two scans

Table 2 recaps the results of the comparison of the 2 studied scans for two grid resolutions (0.5 and 1 m). The total number of Svoxels was calculated for a grid including the circular plot. After merging two scans from different base stations we noticed that the no-data values represented only about 12 % of the total number of Svoxels in the plot for all grid resolutions. The Svoxel centers, for which a significant density index value was computed from both scans, are only about 55 % of the total number of Svoxels of the grid. This low value is explained by the fact that only the bottom part of the plot was scanned in the second scan. The significant differences in the magnitude for the "Mean density index difference" and the "Mean difference for positive and significant density index values" are explained by a high number of Svoxels located in vegetation gaps. These Svoxels, with a null index value, are consistent between scans. Large differences in density index values are observed inside the vegetation elements. For the 50 cm grid resolution about 15 % of the density index values differ from less than 1 % and 45 % from less than 5 % but 20 % of the Svoxels have index values with a difference higher than 20 %. Part of these differences can be explained by (1) the difference between the Svoxel shapes observed from two points of view and (2) by the type of vegetation material hit by the laser beams. For example trunks or large branches can be sources of differences since they are not seen at the same place according to the base station location (back part of them, relative to view point, is occluded). Some differences may also be related to the potential bias we previously

mentioned. All these hypotheses will have to be verified. Merging results from various scans is expected to improve the reliability of the density index. Lastly, we observed from the results that mean differences decrease with resolution while standard deviation increase. This tends to confirm the influence of large wooded elements present in the Svoxel on density index value differences. Actually, when grid resolution is getting coarser the proportion of large wooded elements inside the Svoxel decreases thus reducing the mean difference.

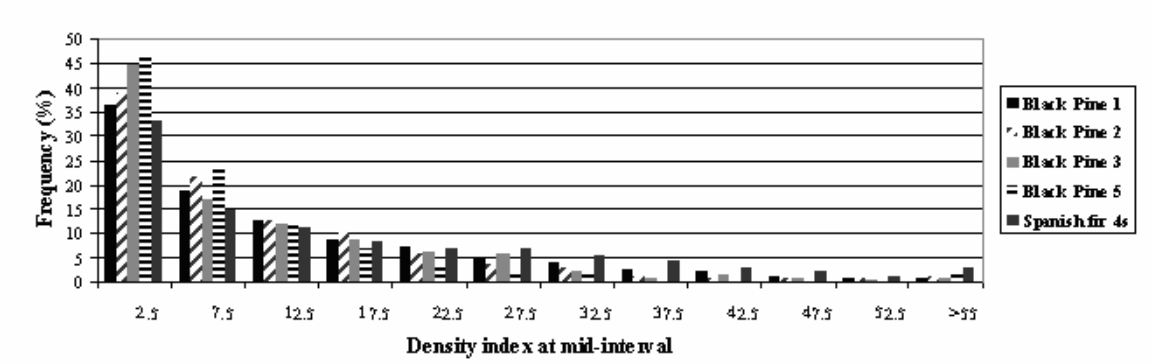

Figure 5: Histograms of density index values (positive and significant) for 5 tree crowns and for a Svoxel resolution of 50 cm.

Table 2: Results of comparison between density index values computed for two scans.

Svoxel resolution	Total number of Svoxel in the grid	**Mean difference of density indices** *(SD)* [Number of Svoxels]			**Mean difference for positive and significant density index values** *(SD)* [Number of Svoxels]		
1 m	58499	-1.4	(6.4)	[432175]	-4.1	(11.5)	[698]
50 cm	467999	**-0.7**	*(5.4)*	[208531]	**-3.1**	*(16.1)*	[2266]

4. Conclusion

We proposed an innovative method to quantify spatial distribution in 3D of forest structure from terrestrial laser scanner data. The method rests on the hypothesis that the amount of laser beam returns inside a Svoxel (volume element defined in the lidar spherical coordinate system) is proportional to the density of vegetation material included inside this Svoxel. First results appeared very promising despite a persisting bias resulting from occlusions. While the density indexes globally confirm our hypotheses, some adjustments are required to improve further the interrelationship between the lidar returns and the amount of forest components in the Svoxels. Future work will focus on improving our algorithm, refining calculations, and correcting biases. In-depth analysis of scans acquired in both first and last pulse modes and multi-scan comparisons and combinations at different grid resolutions also need to be tested out. Our analysis was an essential prerequisite for developing a method aiming at merging the different scans acquired on a same plot. This study was realized considering the prospect of establishing a link between airborne lidar data and field data with the aim of improving information extraction from airborne lidar data on forested areas. These results are very promising for the development of quantitative measures of the 3D forest structure that will meet the actual information needs in the fields related to forest ecology and management.

Acknowledgements:

This research was made possible though funding provided by the Centre National d'Etudes Spatiales (CNES). We are also thankful to the GIS Draix for its logistical support during the fieldwork.

References

Aschoff, T., Thies, M. and Spiecker, H., 2004. Describing forest stands using terrestrial laser-scanning. In, XXth ISPRS Congress. *International Archives of the Photogrammetry, Remote Sensing and Spatial Information Sciences*, Istanbul, July 12-23, pp. 5.

Bienert, A., Scheller, S., Keane, E., Mohan, F. and Nugent, C., 2007. Tree detection and diameter estimations by analysis of forest terrestrial laser scanner point clouds. In: H.H. P. Rönnholm, J. Hyyppä (Editor). *Proceedings of the ISPRS Workshop 'Laser Scanning 2007 and SilviLaser 2007'.* Espoo, September 12-14, 2007, Finland: 50-55.

Danson, F.M., Hetherington, D., Morsdorf, F., Koetz, B. and Allgöwer, B., 2007. Forest canopy gap fraction from terrestrial laser scanning. *IEEE Geoscience and Remote Sensing Letters*, 4(1), 157-160.

Fleck, S., Obertreiber, N.,Schmidt, I., Brauns, M., Jungkunst, H.F., and Leuschner, C., 2007. Terrestrial lidar measurements for analysing canopy structure in an old-growth forest. In: H.H. P. Rönnholm, J. Hyyppä (Editor). *Proceedings of the ISPRS Workshop 'Laser Scanning 2007 and SilviLaser 2007'*. Espoo, September 12-14, Finland: 125-129.

Hopkinson, C., Chasmer, L., Young-Pow, C. and Treitz, P., 2004. Assessing forest metrics with a ground-based scanning lidar. *Canadian Journal of Forest Research*, 34(3), 573-583.

Király, G. and Brolly, G., 2007. Tree height estimation methods for terrestrial laser scanning in a forest reserve. In: H.H. P. Rönnholm, J. Hyyppä (Editor). *Proceedings of the ISPRS Workshop 'Laser Scanning 2007 and SilviLaser 2007'*. Espoo, September 12-14, Finland: 211-215.

Lichti, D.D., Gordon, S.J. and Stewart, M.P., 2002. Ground-based laser scanners: operation, systems and applications. *Geomatica*, 56(1), 21-33.

Lim, K., Treitz, P., Wulder, M., St-Onge, B., and Flood, M., 2003. Lidar remote sensing of forest structure. *Progress in Physical Geography*, 27, 88-106.

Van der Zande, D., Hoet, W., Jonckheere, I., Van Aardt, J., and Coppin, P., 2006. Influence of measurement set-up of ground-based LiDAR for derivation of tree structure. *Agricultural and orest meteorology*, 141, 147-160.

Watt, P.J., and Donoghue, D.N.M., 2005. Measuring forest structure with terrestrial laser scanning. *International Journal of Remote Sensing*, 26(7), 1437-1446.

Wezyk , P., Koziol, K., Glista, M. and Pierzchalski, M., 2007. Terrestrial laser scanning versus traditional forest inventory. First results from the Polish forests. In: H.H. P. Rönnholm, J. Hyyppä (Editor). *Proceedings of the ISPRS Workshop 'Laser Scanning 2007 and SilviLaser 2007'*. Espoo, September 12-14, Finland: 424-429.